arXiv:1006.1815v1 [cond-mat.stat-mech] 9 Jun 2010

Coherent dynamics of macroscopic electronic order through a symmetry-breaking transition.

R.Yusupov,[1] T.Mertelj,[1] V.V.Kabanov,[1] S.Brazovskii,[3],

P.Kusar[1], J.-H.Chu,[2] I. R. Fisher,[2] and D. Mihailovic,[1]

[1]*Dept. of Complex Matter, Jozef Stefan Institute,*

Jamova 39, Ljubljana, SI-1000, Ljubljana, Slovenia

[2]*Geballe Laboratory for Advanced Materials and Department of Applied Physics,*

Stanford University, California 94305, USA and

[3] *LPTMS-CNRS, UMR8626, Univ. Paris-Sud, Bat. 100, Orsay, F-91405 France*

The temporal evolution of systems undergoing symmetry breaking phase transitions (SBTs) is of great fundamental interest not only in condensed matter physics, but extends from cosmology to brain function and finance [1–3, 5]. However, the study of such transitions is often hindered by the fact that they are difficult to repeat, or they occur very rapidly. Here we report for the first time on a high-time-resolution study of the evolution of both bosonic and fermionic excitations through a second order electronic charge-ordering SBT in a condensed matter system. Using a new three-pulse femtosecond spectroscopy technique, we periodically quench our model system into the high-symmetry state, detecting hitherto unrecorded coherent *aperiodic* undulations of the order parameter (OP), critical slowing down of the collective mode, and evolution of the particle-hole gap appearing through the Peierls-BCS mechanism as the system evolves through the transition. Numerical modeling based on Ginzburg-Landau theory is used to reproduce the observations without free parameters. The close analogy with other "Higgs potentials" in particle physics[4] gives new insight into hitherto unexplored dynamics of both single particle and collective excitations through a SBT. Of particular interest is the observation of spectro-temporal distortions caused by disturbances of the field arising from spontaneous annihilation of topological defects, similar to those discussed by the Kibble-Zurek cosmological model[2].

The behaviour of SBTs in many diverse systems is commonly studied under near-equilibrium (near-ergodic) conditions, where excitations on all timescales contribute to the process, and the behaviour of physical quantities through the SBT is described by power laws and critical exponents. However, when the ordering proceeds non-ergodically, the situation is fundamentally different. The quasiparticles and collective boson excitations perceive the homogeneous crystal background as an effective vacuum. Consequently the ordering takes place as a well-defined sequence of events in time. For studying the temporal evolution of elementary excitations through a SBT in condensed matter systems undergoing second order SBTs, crystals with electronically-driven instabilities are perhaps the most suitable. Chosing a prominent example amongst such systems, rare-earth tri-tellurides have an electronic instability caused by a Fermi surface nesting, leading to a second-order transition to a broken symmetry charge-density-wave (CDW) ordered state at low temperature [6–9]. The

CDW state is characterized by spatial modulations $\sim \cos(Qx + \phi)$ of the electronic density and of the lattice displacements which give rise to a complex OP $\Psi \sim \Delta e^{i\phi}$. The elementary bosonic collective excitations of Δ and ϕ are the amplitude and the phase modes (AM and PhM), and Ψ may be viewed as a "Higgs field",[1] opening a gap $2|\Delta|$ in the fermionic spectra. Quasiparticle (QP) and AM excitations in $TbTe_3$ have been recently systematically characterized [10, 11]. In this paper we focus on $TbTe_3$ (T_c = 336 K), but experiments on a number of microscopically diverse systems ($DyTe_3$, 2H-$TaSe_2$ and $K_{0.3}MoO_3$) are also presented demonstrating the range of behavior observed within this universality class of SBTs.

The main idea realised here is to repetitively quench the system into the high symmetry state using a short (50 fs) intense "destruction" (D) laser pulse and then monitor the time evolution of reflectivity oscillations using a pump-probe (P-p) sequence as it freely evolves through the transition (Fig.1a). (The experimental details, including data processing are given in the supplementary information (SI)). The D pulse excites electrons and holes, thus suppressing the electronic susceptibility at $2k_F$ whose divergence is the cause for the CDW formation. Any asymmetry in the band structure also leads to an imbalance of the e and h populations, shifting the chemical potential and causing a disturbance $\delta\vec{q}$ of the Fermi surface $\vec{k}_F$ according to $n_e - n_h \propto \mid \delta\vec{q} \mid /\pi$ and destroying the CDW. Following the quench, after initial rapid quasiparticle (QP) relaxation, we can expect the appearance of topologically nontrivial local configurations - domain walls, solitons. etc. which are allowed by the ground state degeneracy with respect to ϕ [12]. Our technique allows us not only to control and monitor the emergence of elementary excitations and evolution of Ψ with high time-resolution, but permits a unique experimental detection of spatio-temporal field distortions arising from domain wall annihilation events.

Focusing on $TbTe_3$, the evolution of the system after a quench is measured by the transient reflectivity $\Delta R/R$ as a function of $D - P$ time delay Δt_{12} (Fig. 1b)). We can distinctly see an exponential QP transient at short times $\Delta t_{23} < 1$ ps, and an oscillatory response due to AM and coherent phonon oscillations [11] evolving through the SBT. A 2D plot highlighting the QP response is shown in Fig. 2a). We see that immediately after the quench the QP peak amplitude A_{QP} is completely suppressed, indicating the disappearance of a gap. As the QP peak starts to recover, initially the QP lifetime τ_{QP} is quite long (a few ps), but recovers quickly with time. Both A_{QP} and τ_{QP} recover to their equilibrium values within

1-2 ps. A single exponential fit to both τ_{QP} and A_{QP} is shown in Fig 2b), giving the QP gap recovery time $\tau_{\tau_{QP}} = \tau_{A_{QP}} = 650 \pm 50$fs. This is consistent with the previously reported relation $\tau_{QP} \sim 1/\Delta(T)$ [11, 13].

Fig. 1c) shows $\Delta R/R$ for different Δt_{12} with the QP signal subtracted, showing an unusual oscillatory response through the SBT. The Fast Fourier transform (FFT) power spectra of these data as a function of Δt_{12} are plotted in Fig. 2c). The most obvious non-trivial observation in the $\omega - \Delta t_{12}$ plots is that the intensity of the AM fluctuates strongly up to ~ 7 ps. It then gradually saturates with increasing Δt_{12} (not shown). The fluctuations are irregular at first, showing a distinct slowing down in the critical region $\Delta t_{12} = 1.5$ ps. The AM, whose frequency in the equilibrium broken symmetry state is 2.18 THz, shows a dramatic softening for $\Delta t_{12} < 2$ ps. In the course of the system recovery, the AM crosses the 1.75 THz phonon mode, and a Fano interference effect is clearly observed around $t_{12} \simeq 1$ ps, similar to the one observed in the T-dependence.[11] Significantly, the spectra appear strongly distorted around $\Delta t_{12} = 3.5 - 4$ ps, showing *asymmetric diagonal* "blobs". After 6 ps the fluctuations die down and the AM intensity eventually reaches full amplitude in approximately 60 ps without any significant change in linewidth and frequency (not shown).

To model the evolution of the system through the SBT, we describe the field Ψ using a non-linear weakly dispersive Ginzburg-Landau (GL) model. Neglecting phase fluctuations[14], the potential energy of the system can be described by a double-well, rather than a "Mexican hat" potential:

$$U = \int dz \left(-\frac{1}{2}(1-\eta)A^2 + \frac{1}{4}A^4 + \frac{1}{2}\xi^2 \left(\frac{\partial A}{\partial z} \right)^2 \right) \tag{1}$$

whose time-dependence is shown schematically in Fig. 3a. Here $A(t,z) = \Delta(t,z)/\Delta_{eq}$ is the time-space dependent amplitude of Ψ, normalized to the equilibrium value Δ_{eq}, and ξ is the coherence length coupling regions of different z. The function $1 - \eta(t,z)$ is a parameter describing the perturbation, akin to the temperature deviation $(T - T_c)$ from criticality in usual GL theory. For spatially uniform $A(t)$, $\eta(t) = \eta(0)\exp(-t/\tau_{A_{QP}})$ as plotted in Fig. 3b). Its exponential form and the parameter $\tau_{A_{QP}}$ are experimentally determined from fits to Fig. 2b). The time-evolution of U and $\mu = 1 - \eta$ with $\eta(0) = 2$ is shown schematically in Fig. 3a): Before the D pulse, and for large t or z, $\eta = 0$, so the system resides in a homogeneously ordered ground state with $|A| = 1$. Immediately after the D pulse, $1 - \eta < 0$ and the double well potential disappears in favor of a single energy minimum at $A = 0$.

As $1-\eta$ increases and becomes positive, nonzero minima emerge at $\pm A_{min} = \pm(1-\eta)^{1/2}$, and start to attract the system, which is soon trapped in one of them, and the symmetry is broken again. From Eq. [1], the equation of motion can then be written as:

$$\frac{1}{\omega_0^2}\frac{\partial^2}{\partial t^2}A + \frac{\alpha}{\omega_0}\frac{\partial}{\partial t}A - (1-\eta)A + A^3 - \xi^2\frac{\partial^2}{\partial z^2}A = 0 \tag{2}$$

Here ω_0 is the angular frequency of the bare ($2k_F$) phonon mode responsible for the CDW formation; the second term describes its damping $\alpha \leq \Delta\nu_{AM}/\nu_{AM}$. The exponentially decaying light intensity due to the finite penetration depth of light is accounted for by the excitation function $\eta'(t,z) = \eta(t)\exp(-z/\lambda)$ where λ=20 nm is the light absorption depth of $TbTe_3$ at 800 nm. Using the experimental values for τ_{QP}, $\nu_{AM} = \tilde{\omega}_0/2\pi = 2.18$ THz, the linewidth $\Delta\nu_{AM} = 0.2$ THz, coherence length $\xi = 1.2$ nm [8] and penetration depth $\lambda = 20$ nm, there are no free parameters and we can compute $A(t,z)$. In Fig. 3b) we first plot the spatially homogeneous solution with $\xi = 0$, with and without the P pulse. In this particular simulation, the parameters were chosen to illustrate that a small perturbation of the P pulse causes the system to revert to a different minimum. With many preceding oscillations, the final ground state is ergodically uncorrelated with the initial one, hence the formation of domains is expected under inhomogeneous conditions.

The full inhomogeneous solution $A(t,z)$ to Eq. 2 is plotted in Fig. 4a). We see that after ~ 1 ps, four domains are formed parallel to the surface with $A(t,z)$ oscillating either around 1 or -1 (orange or blue respectively), accompanied by the emission of $A(t,z)$-field waves, which propagate into the sample. At ~ 3 ps we observe the fusion of two domain walls, which is accompanied by the emission of field waves of $A(t,z)$ now propagating towards the surface *and* into the bulk (arrows). They appear to reach the surface around $\Delta t_{12} \simeq$ 4-5 ps which - as we shall see - cause detectable distortions of the spectra at around 5-6 ps. The appearance of such A-waves following annihilation is qualitatively robust with respect to the parameter values for $TbTe_3$ (see SI). (More A-field wave dynamics is shown in the accompanying movies.)

The calculated reflectivity response detected by the probe p is given by the difference between the response *with* and *without* the pump P pulse: $\Delta R(t,\Delta t_{12}) \propto \int_0^\infty [A_D^2(t,z) - A_{DP}^2(t,z,\Delta t_{12})]e^{-z/\lambda}dz$, where $A_{DP}^2(t,z,\Delta t_{12})$ is calculated replacing $\eta \rightarrow \eta_P(t) = \eta(0)\exp(-t/\tau_{sp}) + \Pi\Theta(t-t_{12})exp[-(t-t_{12})]/\tau_{sp})$. The exponential term accounts for the probe penetration depth. The typical value of $\Pi = 0.1$, where Π is the P pulse

intensity relative to the D pulse and $\Theta(t - t_{12})$ is a unit step function (see SI for details). The calculated response for the homogeneous solution $\Delta R(t, \Delta t_{12})$ is shown by the green curve in Fig. 3b).

In Fig. 4b) we show the FFT power spectra from $\Delta R(t, \Delta t_{12})$ taking full account of spatial inhomogeneity for D, P and p. The main features of our data in Fig. 2c) are unmistakably present: oscillations of $A(t)$ are clearly visible at short times, as well as the hallmark of the transition itself, namely the critical slowing of the AM oscillations close to the critical point $t_c \simeq 1.5$ ps, pinpointing the exact critical time of the transition t_c. At this bifurcation point topological defects are formed. The calculation also reproduces the softening of the AM for $\Delta t_{12} < 2$ ps. After 2ps, the ripples in $A(t, z)$ discussed above cause a temporal deformation of the spectral profiles, giving diagonal blobs at $5 \sim 6$ ps shown in Fig. 4b). These are remarkably similar to the diagonal spectral distortions observed in the experimental data in Fig. 2c). A summary of exhaustive modeling within a wide parameter space is presented in the SI showing that inhomogeneity without A-field waves cannot cause diagonal deformations, only vertical ones. The diagonal distortions in $\omega - t_{12}$ plots are thus unambiguously attributed to the A-field waves created upon the annihilation of defects.

Identical experiments on three additional microscopically diverse systems (*2H*-$TaSe_2$, $K_{0.3}MoO_3$ and $DyTe_3$) displaying a 2nd order SBT presented in the SI show that the sequence of events after the quench: *(i) ultrafast QP gap recovery* $\rightarrow$ *(ii)* Ψ*-field amplitude fluctuations* $\rightarrow$ *(iii) critical slowing down through* t_s *and (iv) domain creation* $\rightarrow$ *coherent defect annihilation* is commonly observed in systems which unambiguously belong to the same universality class (the tellurides and the selenide). The microscopic properties of the underlying vacuum such as λ and ξ change the details. $K_{0.3}MoO_3$ - which already shows lack of AM softening in the T-induced transition[13]- does not show step (iv), which we attribute to departure from universality. It is interesting to note that the mechanism described here for topological defect creation is conceptually and historically related not only to vortex formation in superconductivity, but also to the Kibble-Zurek mechanism for the formation of cosmic strings. The $A(t, z)$ -waves such which we observe after annihilation events have a direct analogue in the Higgs spontaneous symmetry breaking mechanism. All these models share a common underlying potential, albeit with different symmetries of OP and microscopic properties of the underlying vacuum[1, 2, 4, 15]. A notable distinction of our system is that ϕ relaxation is slow compared to the relaxation of the potential itself,

allowing the collective mode and topological defect dynamics to be clearly observed. In superconductors, the QP relaxation is beautifully observed[16], but the collective mode is overdamped and unobservable[17]. Thus real-time observations and coherent control of the macroscopic order through the SBT appears to be a rather unique feature of femtosecond laser experiments on CDW systems.

Acknowledgments. We wish to thank Christoph Gadermaier for critial reading of the manuscript. Work at Stanford University supported by the Department of Energy, Office of Basic Energy Sciences under contract DE-AC02-76SF00515. S.B. acknowledges the support from the ANR project BLAN07-3-192276.

---

[1] Topological defects and the Non-Equilibrium Dynamics of Symmetry-Breaking Phase Transitions, NATO ASI Series, ed. Yu.M. Bunkov and H. Godfrin, Kluwer Academic Publishers, (2000).

[2] Kibble, T.W.B.,Topology of cosmic domains and strings. *J Phys A-Math Gen* **9**, 1387-1398 (1976), Zurek, W.H., Cosmological experiments in superfluid helium?. *Nature* **317** 505-507 (1985).

[3] Eltsov, V.B., Krusius, M., and Volovik, G.E., Vortex formation and dynamics in superfluid ^{3}He and analogies in quantum field theory, *Progress in Low Temperature Physics*, **15**, 1-137 (2005).

[4] P.W. Higgs, Spontaneous symmetry breakdown without massless bosons. Physical Review **145**, 1156 (1966),

[5] Perlovsky, L.I. and Kozma, R., Neurodynamics of cognition and consciousness, Springer (2007); Sornette, D., Why Stock Markets Crash: Critical Events in Complex Financial Systems, Princeton University Press (2002).

[6] Dimasi, E., et al., Chemical pressure and charge-density waves in rare-earth tritellurides. *Physical Review B* **52**, 14516-14525 (1995).

[7] Ru, N., and Fisher, I.R., Thermodynamic and transport properties of YTe_3, $LaTe_3$, and $CeTe_3$. *Phys. Rev. B* **73**, 033101-1 - 033101-4, (2006)

[8] Ru, N., et al., Effect of chemical pressure on the charge density wave transition in rare earth tritellurides RTe3, *Phys. Rev. B.* **77**, 035114 (2008), Fang, A., et al., STM Studies of TbTe3:

Evidence for a Fully Incommensurate Charge Density Wave, *Phys. Rev. Lett.* **99**, 046401-1 - 046401-4 (2007).

[9] Brouet, V., et al., Fermi surface reconstruction in the CDW state of CeTe3 observed by photoemission, *Phys. Rev. Lett* **93**, 126405 (2004); Laverock, J., et al., Fermi surface nesting and charge-density wave formation in rare-earth tritellurides. *Physical Review B* **71**, 085114-1 - 085114-5 (2005).

[10] Schmitt, F., et al., Transient Electronic Structure and Melting of a Charge Density Wave in $TbTe_3$, *Science* **321** 1649-1652 (2008).

[11] Yusupov, R., et al., Single-Particle and Collective Mode Couplings Associated with 1- and 2-Directional Electronic Ordering in Metallic RTe_3 (R =Ho; Dy; Tb). *Phys. Rev. Lett.* **101**, 246402-246404 (2008).

[12] Brazovskii, S., Solitons and Their Arrays: from Quasi One-Dimensional Conductors to Stripes, *J. of Superconductivity and Novel Magnetism*, **20**, 489 (2007).

[13] J. Demsar et al., Single particle and collective excitations in the one-dimensional Charge Density Wave solid $K_{0.3}MoO_3$ probed in real time by femtosecond spectroscopy *et al.*, *Phys.Rev. Lett.* **83**, 800-803 (1999).

[14] Phase perturbations can be neglected on short timescales, because they require significant time for nucleation.

[15] C.M.Varma. Higgs boson in superconductors. J Low Temp Phys. **126**, 901 (2002)

[16] J.Demsar et al., Superconducting Gap Δ_c, the Pseudogap Δ_p, and Pair Fluctuations above T_c in Overdoped $Y_{1-x}Ca_xBa_2Cu_3O_{7-\delta}$ from Femtosecond Time-Domain Spectroscopy, *Phys. Rev.Lett.* **82**, 4918 (1999) and many others.

[17] L. P. Gorkov and N. B. Kopnin, Usp. Fiz. Nauk 116, 413 (1975) [Sov. Phys. Usp. 18, 496 (1976)

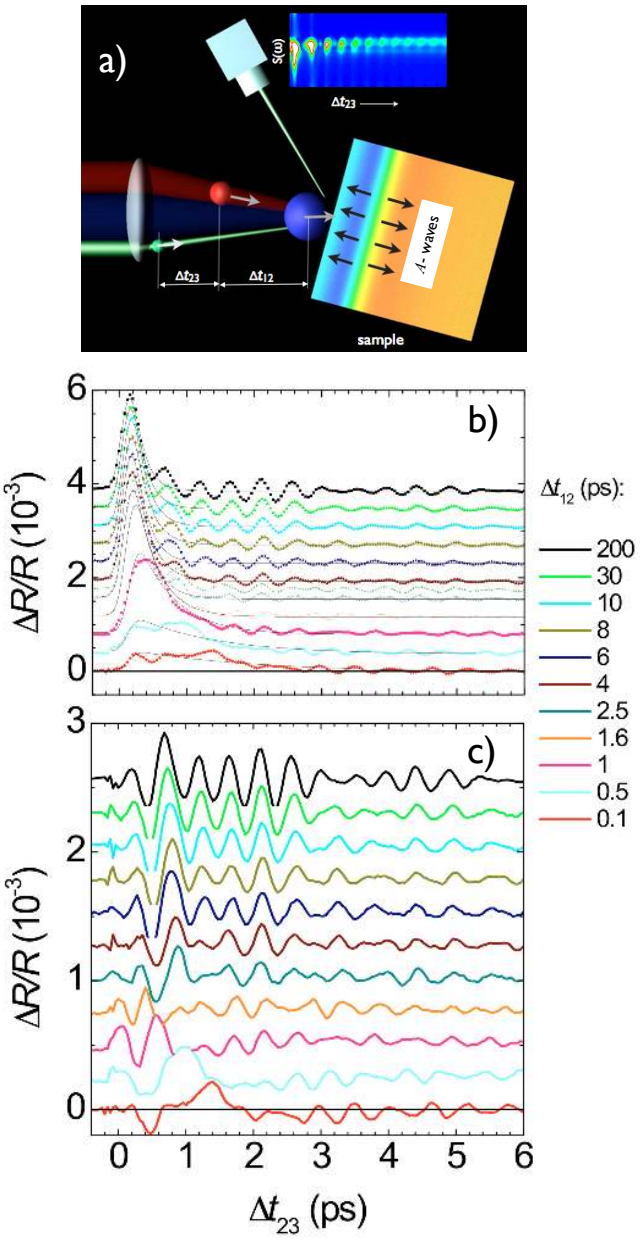

Figure 1: a) A schematic diagram of the timing of the laser pulses: a *destruction* (D) pulse (represented by the blue ball) quenches the system, while a *pump-probe* (P-p) sequence probes the reflectivity at a later time Δt_{12}. P and p pulses are represented by red and green balls respectively. b) Raw transient reflectivity data $\Delta R/R$ for different delays $\triangle t_{12}$ (displaced vertically), showing a QP peak at short times, and OP and coherent phonon oscillations at longer times c) $\Delta R/R$ with the QP response subtracted.

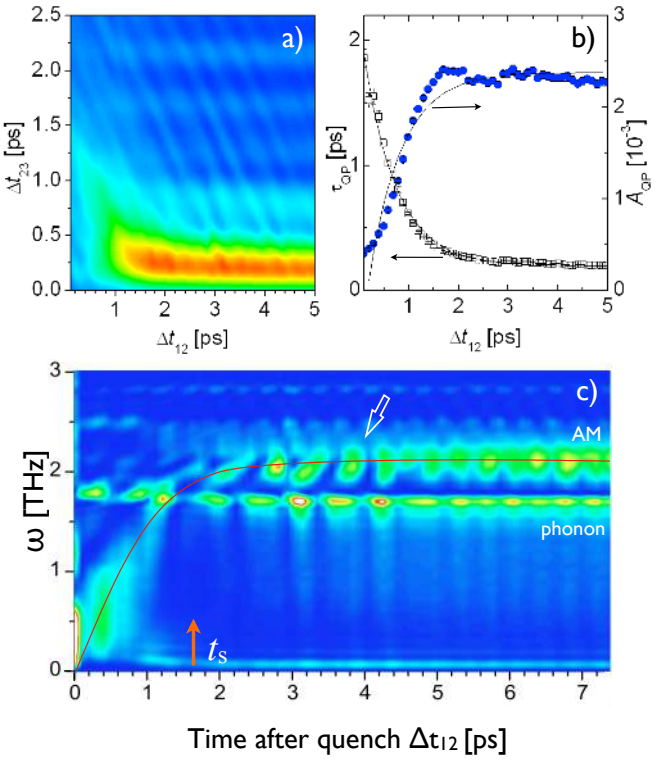

Figure 2: $|\Delta R/R|_{QP}$ after the quench as a function of Δt_{12}, (Note the ripples arising from coherent oscillations of the OP.) b) The QP lifetime τ_{QP} and the amplitude of the QP response A_{sp} as a function of Δt_{12}. A single exponential fit to both data sets (shown by the lines) gives $\tau_{\tau_{QP}} = \tau_{A_{QP}} = 650 \pm 50$fs. c) The FFT power spectra of the data in Fig. 1 c) as a function of Δt_{12} recorded at 100 fs intervals. Note the non-periodic fluctuations of intensity at around the transition (1.5 ps) and the strongly asymmetric space-time lineshapes for $\Delta t_{12} = 2 \sim 4$ ps (white arrow). The orange arrow indicates the critical time of the SBT. The red line is a superimposed plot of a fit to the QP decay from b) above.

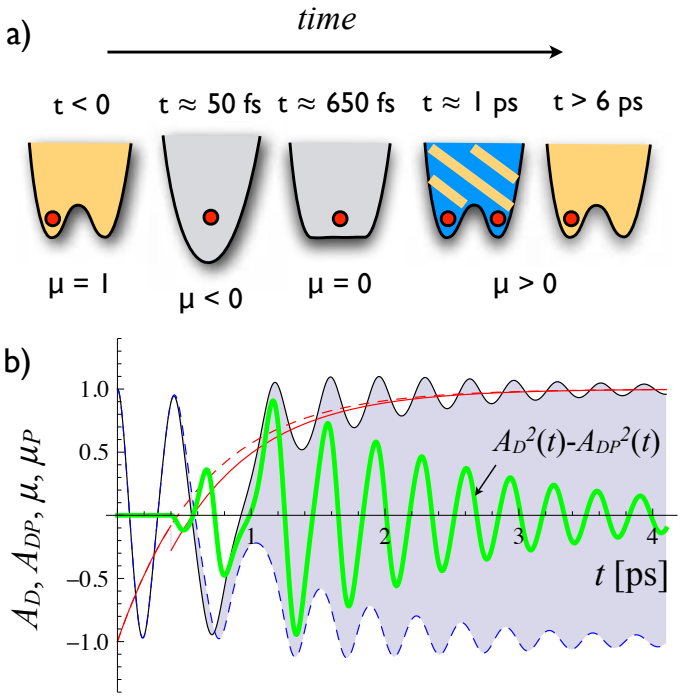

Figure 3: a) The evolution of the potential U (Eq.1) as a function of time. The system is in the high symmetry state (grey) at very short times after the quench. The red dot signifies the state of the system, while the blue/orange potential signifies a topologically mixed broken-symmetry state. b) The time-dependence of the control parameters $\mu(t) = 1 - \eta(t)$ (solid red) and $\mu_P(t)$ (dashed red) calculated with the experimental value of $\tau_{A_{sp}} = 0.65 \pm 0.05$ ps for$\triangle t_{12}$=0.4 ps. The predicted oscillations of $A(t)$ *with* and *without* the P pulse are shown by the dashed and solid oscillatory blue curves respectively. The predicted optical response $\Delta R(t)$ is shown by the green curve.

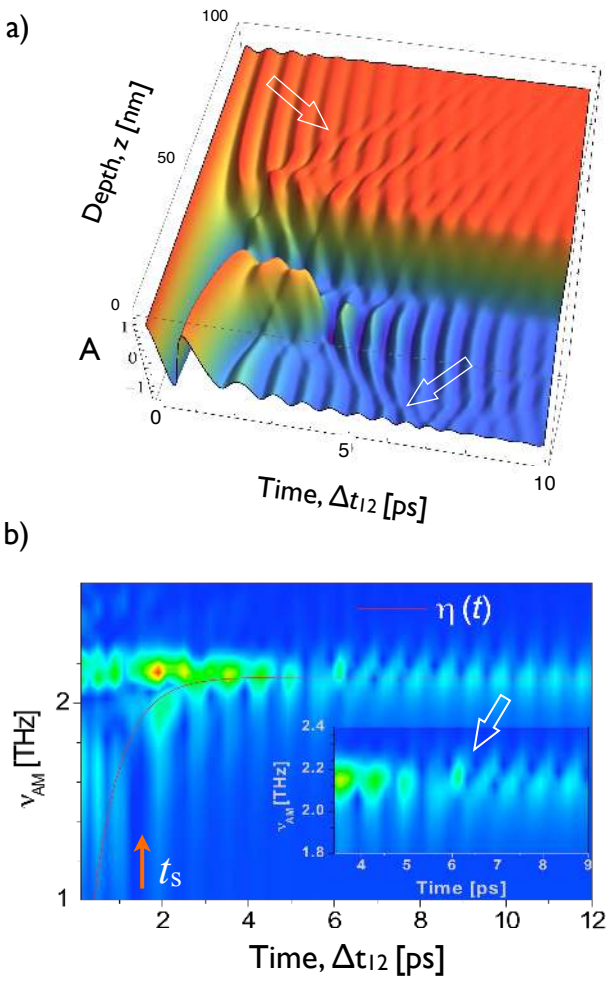

Figure 4: a) The calculated $A(z,t)$ as a function of depth z and Δt_{12}. Note the ripples in caused by the annihilation event at ∼3.5 ps (arrows). b) The corresponding computed transient reflectivity $\Delta R(z,t)$ as a function of Δt_{12}. Note the predicted diagonal distortion due to the $A(z,t)$-wave reaching the surface, indicated by the white arrow. The orange arrow points to the critical slowing down at the critical time of the transition t_c, i.e. the bifurcation point. The thin red line shows the function $\eta(t)$.